Formulation and additive manufacturing of polysaccharide-surfactant hybrid gels as gelatin analogues in food applications

Fenton, Thomas; Daffner, Kilian; Mills, Tom; Pelan, Eddie; Gholamipour Shirazi, Azarmidokht

DOI:
10.1016/j.foodhyd.2021.106881

Document Version
Peer reviewed version

Citation for published version (Harvard):
Fenton, T, Daffner, K, Mills, T, Pelan, E & Gholamipour Shirazi, A 2021, 'Formulation and additive manufacturing of polysaccharide-surfactant hybrid gels as gelatin analogues in food applications', *Food Hydrocolloids*, vol. 120, 106881. https://doi.org/10.1016/j.foodhyd.2021.106881

Formulation and additive manufacturing of polysaccharide-surfactant hybrid gels as gelatin analogues in food applications.

Thomas Fenton, Azarmidokht Gholamipour-Shirazi, Kilian Daffner, Tom Mills, Eddie Pelan

TFF710@student.bham.ac.uk

Department of Chemical Engineering, University of Birmingham, Birmingham, B15 2TT, United Kingdom

Abstract

A vegetarian alternative to gelatin, for use in food applications was proposed as a synergistic combination of 0−2 wt% low acyl gellan gum (LAG) and 0−2 wt% tamarind seed xyloglucan (TSX). The mechanical, thermal and temperature-mediated release properties of the gels were examined using rheology and conductivity. The influence of the addition of a food grade emulsifier, Tween® 20, was also investigated. It was found that both the total concentration of biopolymers and the ratio of polymer blends influenced thermal (gelling and melting temperatures) and mechanical (storage modulus and phase angle) properties, however the total polymer concentration was the major factor. The addition of Tween® 20 led to small increases gelling and melting temperatures, elastic modulus and a small reduction phase angle in most of the LAG/TSX samples. Using rheological data the LAG/TSX samples were predicted to be printable using extrusion-based additive manufacturing, which was then performed on a custom-made printer. The rheological and release data suggested that 0.5 wt% LAG/1.5 wt% TSX/1 wt% Tween® 20 was the most similar to a tested sample of 5 wt% porcine gelatin in terms of viscoelastic moduli, gelling & melting temperatures and release profile, and could therefore be developed as a printable gelatin replacement. No difference was found between the release properties of moulded versus printed gels.

1. Introduction

Across many industries, notably the food and pharmaceutical industries, there is a need for the development of vegetarian gels that provide 'melt-in-the-mouth' behaviour (Ikeda & Talashek, 2007), as an alternative to porcine gelatin-based formulations. This due to concerns over gelatin's animal-

based origins. Additionally, the junction zones in gelatin continually re-arrange to become gradually more thermally stable, hence the gel strength and melting temperature of gelatin is a direct function of its age (Ledward, 2000). Gelatin alternatives must be firm at room temperature yet must soften significantly at body temperature (37 °C) to provide the correct mouthfeel and release properties. In such edible formulations it is often advantageous to include an emulsifier to allow for the stable inclusion of oil-based flavourings and additives (Kralova & Sjöblom, 2009). Initial characterisation of a gel-surfactant system would pave the way for future gel-oil-surfactant formulations for the food industries and beyond.

Gellan gum is an extracellular polysaccharide secreted by *Sphingomonas elodea* (syn. *Pseudomanos elodea*) micro-organisms (Moorhouse, Colegrove, Sandford, Baird, & Kang, 1981). Its primary structure consists of a linear repetition of four saccharide derivatives: →3)-β-D-Glcp-(1→4)-β-D-GlcpA-(1→4)-β-D-Glcp-(1→4)-α-L-Rhap-(1→ (Jansson, Lindberg, & Sandford, 1983). In its native high acyl form, the polymer has two acyl substituents present on the 3-linked glucose (Kuo, Mort, & Dell, 1986), however these can be removed through heating under alkaline conditions to yield the deacylated (low acyl) form (Chilvers & Morris, 1987). Both gellans undergo gelation in the presence of sufficient gelling cations through the formation and subsequent aggregation of double helices, achieved by hydration at an elevated temperature followed by cooling (Grasdalen & Smidsrød, 1987). The degree of acyl substitution determines the resultant gel properties: high acyl gellan (HAG) gum typically forms thermoreversible, soft, elastic gels whereas low acyl gellan (LAG) gum generally forms non-thermoreversible, hard, brittle gels (Lee, Fisher, Kallos, & Hunter, 2011). Divalent cations are much more effective at promoting gelation in gellan compared to monovalent cations (Grasdalen & Smidsrød, 1987).

Tamarind seed xyloglucan (TSX) is a non-ionic, branched polysaccharide which is extracted from the seed of the tamarind tree *Tamarindus indica* (Kaur, Yadav, Ahuja, & Dilbaghi, 2012; Nayak, Pal, & Santra, 2014). TSX has a backbone of (1→4)β-D-glucans substituted with side chains of α-D-

xylopyranose which are linked (1→6) to glucose molecules (Kaur et al., 2012). In water, TSX swells and causes a rise in viscosity which sees it used mainly as a thickener and stabiliser in the food industry (Nayak et al., 2014), however, it does not form a gel on its own.

A synergistic combination of two biopolymers describes a case whereby a mixture of polymers shows different properties than what is possible from any of the individual substituent polymers. The origin of this synergistic effect is due to the formation of either a phase-separated or a coupled network, depending on whether direct binding takes place or not between the two polymers. In either case a synergistic effect is often indicated by the viscosity of a mixture being greater than the sums of the viscosities of its substituents (Nishinari, Kim, Fang, Nitta, & Takemasa, 2006). Morris (1995) noted that many synergistic interactions arise from mixtures of a polysaccharide that undergoes a coil-helix transition, such as carrageenan, xanthan gum and gellan gum, mixed with another polysaccharide with a β(1→4) linked cellulosic backbone, such as locust bean gum, konjac glucomannan or tamarind seed xyloglucan (Nishinari et al., 2006). Work by Grisel *et al.* (2015), who investigated the synergistic interactions between xanthan and galactomannans, suggested that the mechanism of synergy between the two polymers is dependent on the degree of compatibility between the two molecular structures: in the attractive scenario, unsubstituted areas on the galactomannan can interact with linear, non-helical regions on the xanthan which allows the formation of hybrid junction zones, whereas if the structures are geometrically incompatible, then such junction zones cannot form, and instead the synergy results from a repulsive, phase-separated microstructure.

In an unmodified state, both HAG and LAG have a melting temperature that far exceeds the target for a gelatin replacement (T_m > 70 °C). The synergistic combination of LAG with TSX has been briefly reported in the literature previously (Nayak et al., 2014; Nishinari et al., 2006; Nitta et al., 2003), however its use as a potential gelatin replacement has not been exploited to the authors' knowledge. Ikeda *et al.* (2004) attempted to elucidate the nature of the interaction between TSX and LAG using rheology and atomic force microscopy (AFM). It was found that by mixing two non-gelled mixtures of

LAG and TSX, a gel network was formed, however it could not be definitively stated if this synergism was the result of phase separation or coupling between the polymers. Nitta *et al.*, (2003) also reported synergy between LAG and TSX as detected by rheology and differential scanning calorimetry, but once again, mechanistically the nature of the interaction was not defined.

Surfactants are used widely in edible formulations, primarily as an emulsifier to allow the stable inclusion of hydrophobic additives, such as fats, flavourings and colourings, to water-based formulations (Kralova & Sjöblom, 2009). Polysorbate 20, or Tween® 20, is a non-ionic surfactant widely used as an additive in foodstuffs to stabilise oil-in-water emulsions (Genot, Kabri, & Meynier, 2013). Generally, non-ionic surfactants are preferred in edible formulations due to their low toxicity compared to their charged counterparts (Fasolin, Picone, Santana, & Cunha, 2013). It has generally been reported that charged biopolymers, such as gellan, and polysorbates do not associate (Fasolin et al., 2013) even up to concentrations of 10% w/v, except for chitosan-polysorbate 80 which formed structures on a nanometre and micrometre scale at extremely low (below 0.01% w/v) and extremely high (above 50% w/v) surfactant concentrations (Picone & Cunha, 2013). However, new studies have indicated that non-ionic surfactant micelles can contribute to electrostatic shielding of gelling biopolymers through weak hydrophobic interactions (Yang & Pal, 2020).

Additive manufacturing (3D printing) has recently found its way in food applications (Lipton, Cutler, Nigl, Cohen, & Lipson, 2015; Sun, Peng, Yan, H Fuh, & Soon Hong, 2015; Fan; Yang, Zhang, & Bhandari, 2017). Among the current 3D printing methods for food applications (Chia & Wu, 2015; Guo & Leu, 2013), extrusion is a prevailing technique because it is easy to develop and it has the broadest set of 'inks' (Guvendiren et al., 2016; Tan, Toh, Wong, & Lin, 2018) which can be tailored to match certain rheological requirements (Daffner et al., 2021; Godoi, Prakash, & Bhandari, 2016). Among all the available extrusion techniques, cold extrusion 3D food printing has emerged as the technology which enables the manufacture of food in different compositions, textures, tastes or shapes, and offers huge potential for personalised food products beyond what is achievable with conventional moulding.

However, the high cost of production compared to existing manufacturing techniques is a barrier to commercialisation of 3D printing (Godoi et al., 2016). Warner, Norton and Mills (2019) reported that due to the slow gelation time of gelatin, 3D printing of gelatin-based formulations, without a gelation accelerant, results in distortion of printed shapes after printing. Hence, the development of a printable gelatin analogue would be advantageous.

This study aimed to explore LAG and TSX, firstly as a gelatin replacement, and secondly as an 'ink' to manufacture 3D printed gelled structures. The influence of a common food-grade emulsifier, Tween® 20, was also investigated. Rheology gave information on the thermal and mechanical properties of the gels through temperature and frequency sweeps. The release performance of the gels was measured with respect to temperature in water using conductivity – made possible due to the efflux of cations upon gel erosion. The release profiles from both quiescent and 3D printed gels were compared.

2. Experimental

2.1 Materials

Kelcogel® F (batch 8F0778A), a commercially available low acyl gellan gum was kindly gifted by CP Kelco (USA). Tamarind seed xyloglucan (batch UG660FJ) was purchased from Tokyo Chemical Industry (UK). Gelatin from porcine skin (batch BCBH5042V, 240 - 270 g bloom, type A) was purchased from Sigma Aldrich (Germany). Tween® 20 was purchased from Merck (Germany). All materials were used as received without further purification or modifications. The ion content of Kelcogel® F and tamarind seed xyloglucan was determined by Inductively Coupled Plasma-Optical Emission Spectroscopy (PerkinElmer Optima 8000) as shown in Table 1.

Table 1 – Ion content for polysaccharide samples. Values given are mean averages from at least three successive measurements and the associated standard deviation. (= negative values for ion contents were generated due to the fact that the concentration was below the detectable limits, hence these values can be considered to be 0).*

	Ion content (10^5 × % w/w)			
	Na^+	K^+	Mg^{2+}	Ca^{2+}
Kelcogel® F	31.31 ± 0.08	229.9 ±1.8	2.906 ± 0.473	6.908 ± 0.847
TSX	2.427 ± 0.064	3.283 ± 0.072	-0.472 ± 0.020*	-0.847 ± 0.028*

2.2 Methods

2.2.1 Preparation of gel solutions

Polymer powders were weighed (wet basis) and were slowly added to a vessel of deionized water (Milli-Q, Millipore®) at 80 °C under agitation from a magnetic stirrer bar at a moderate speed to avoid clumping. The flask was covered to prevent evaporation and was kept isothermal under agitation for several hours until no powder clumps remained, and the solution was homogeneous. If required, Tween® 20 was then added dropwise and stirred for 10 minutes under gentle agitation to minimise foaming. Solutions were then stored overnight at room temperature (20 °C) until testing, at which time they were re-heated to 80 °C under gentle agitation. The total concentrations of biopolymers tested were 1 – 3 wt%, and surfactant concentrations were 0 – 1 wt%.

2.2.2 Rheological measurements

An MCR 302 rheometer (Anton Paar, Austria) equipped with a PP50-TG parallel plate geometry (D = 50.0 mm) and a P-PTD200/62/TG lower plate geometry (D = 62 mm) was used to characterise the rheology of the samples. In all measurements, samples were loaded in liquid form at 80 °C and trimmed to a gap of 1 mm, with the geometry pre-heated to 60 °C to avoid pre-gelation ($\delta > 45°$). A thin layer of silicone oil was immediately added to the outer edge of the samples to prevent evaporation and a Peltier hood (H-PTD-200) was lowered. For the amplitude and frequency sweep

measurements the temperature of the geometry was reduced to 20 °C and held isothermally for 5 minutes before proceeding.

2.2.2.1 Amplitude sweep to determine the linear viscoelastic region (LVR)

An amplitude sweep was performed from 0.01 to 100% strain, at a frequency of 6.28 rad s^{-1} (1 Hz) and a temperature of 20 °C. The linear viscoelastic region was determined as the range of strain values which showed no significant degradation (± 1%) in the value of the storage modulus (G').

2.2.2.2 Temperature sweep to determine the gelling and melting temperatures

A temperature sweeps was performed from 60 °C to 10 °C and back to 60 °C for each sample, in triplicate. The applied strain was 1% as this was found to be within the LVR of the samples and all sweeps were performed at a frequency of 6.28 rad s^{-1} (1 Hz). The rate of temperature change was 1 °C per minute. Gelling and melting temperatures were determined by the crossover of the elastic (G') and viscous (G'') modulus.

2.2.2.3 Frequency sweep to determine the mechanical spectra and printability

A frequency sweep was performed in triplicate, with the frequency varying between 62.8 rad s^{-1} to 0.628 rad s^{-1} (10 Hz to 0.1 Hz), at a strain of 1%. The measurements were performed at 20 °C.

2.2.1 3D Printing

A custom-built food 3D printing system was used in this study to conduct extrusion-based printing. 3D digital design of the object was generated with Cura 15.04.6 (Ultimaker B.V., Netherlands). A 10 mL syringe and a 22G needle (inner diameter 0.413 mm) were used for all samples. The syringe was filled with liquid samples (80 °C). All samples were printed at a flow level of 60% (Derossi et al., 2018). The cubes (15 mm × 15 mm × 15 mm) were printed for printability assessment. All objects were printed at a printing bed temperature of 50 °C.

2.2.2 Release Measurements

A SevenEasy conductivity meter (Mettler Toledo, USA) was used to monitor conductivity. Gel cubes (dimensions 15 mm × 15 mm × 15 mm) were formed in a custom 3D-printed mould by pouring liquid samples (50 °C) in to the mould recess, covering with plastic film and were then stored at room temperature overnight in an air-tight container before measurement. The bottom portion and sides of the mould were wrapped in Parafilm® M tape to prevent sample leakage through the slightly porous plastic. A 1 litre beaker was filled with 900 mL of distilled water and a custom 3D printed lid was placed on top of the beaker. The lid contained holes, through which a conductivity probe and a temperature probe were inserted, and a net which extended down in to the beaker for placement of the gel cubes. The beaker was placed on a stirrer hotplate and the water was kept isothermal at either 20, 30 or 40 °C. The water was agitated gently at a constant rate of 100 rpm with a 70 mm pivoted PTFE stirrer bar. Conductivity was logged via Mettler Toledo LabX Direct-pH software, which recorded the measured conductivity once per second until it was manually stopped. The endpoint of the release measurement was determined once the conductivity value was steady (± 0.01 mS cm^{-1}) for 5 minutes.

2.2.3 Statistical Analysis

Data was analysed by calculating the Pearson correlation coefficient (ρ): the further the value of ρ from 0 indicates a strong positive or negative correlation, depending on if the value of ρ is positive or negative respectively. Data was fitted using the linear regression analysis and data populations were compared using two-sample T-tests: both in the Analysis Toolpak for Microsoft Excel. A linear fit was assumed statistically accurate if $R^2 \geq 0.90$ and populations were considered statistically different if P(one-tail) ≤ 0.05. Non-linear regression was performed using the curve fitting tool in SigmaPlot 14.5, and a fit was assumed accurate if $R^2 \geq 0.90$.

3. Results

3.1 Rheology

3.1.1 Temperature sweeps to determine the gelling and melting temperatures

The values of the gelling (T_g) and melting (T_m) temperatures of LAG/TSX gels were obtained as a function of total polymer concentration (at a constant polymer ratio) and a function of polymer ratio (at a constant total polymer concentration). The addition of 1 wt% Tween® 20 on the value of the gelling and melting temperatures was also investigated. All of these data are shown in Figure 1.

In general it was found that the values of the gelling and melting temperatures increased with total biopolymer concentration ($\rho = 0.99$ and 0.90 respectively): at 1 wt% these values were ca. 24 °C and ca. 27 °C, increasing up to ca. 34 °C and ca. 39 °C at 2.5 wt% respectively.

At a total biopolymer concentration of 3 wt%, there was no crossover of the viscoelastic moduli detected in the heating step of the temperature sweep i.e. the gel samples did not melt in the experimental temperature range. The increase in gelling temperature values with the total biopolymer concentration has a good linear fit ($R^2 = 0.99$), however this is untrue for melting temperatures ($R^2 = 0.81$), likely due to the discontinuous rise in T_m at 2.5 wt% total polymer concentration. The introduction of Tween® 20 led to statistically significant increases in the gelling temperatures (ca. 2 °C), and the melting temperatures (ca. 5 °C) as indicated by P(one-tail) = 0.005 and 0.03 respectively. The increase in gelling temperature upon addition of surfactant was independent of total biopolymer concentration ($\rho = -0.24$) yet the melting temperature was found to be dependent ($\rho = 0.92$), hence indicating that the surfactant had a greater influence on the melting temperature of more concentration formulations.

In the second set of data shown in Figure 1, the total biopolymer concentration was kept constant at 2 wt% and the polymer blend was varied: this concentration was chosen as it was a sensible value based on the previous data set. At 0% LAG content, i.e. 100% TSX content, no gelling or melting was

227 detected, and at and beyond 75% LAG content, no melting was detected, hence there are no data at
228 these points. Increasing the LAG content from 25% to 50% only lead to a very small increase in the
229 values of the gelling temperature (ca. 1 °C), and the melting temperature remained constant,
230 indicating very similar gel microstructures. However, as the LAG content was then increased to 75%
231 and 100%, the gelling temperatures increased dramatically (ca. 10 °C per additional 25% LAG) and the
232 melting temperatures increased to beyond the experimental maximum temperature (60 °C),
233 indicating a significant microstructural change

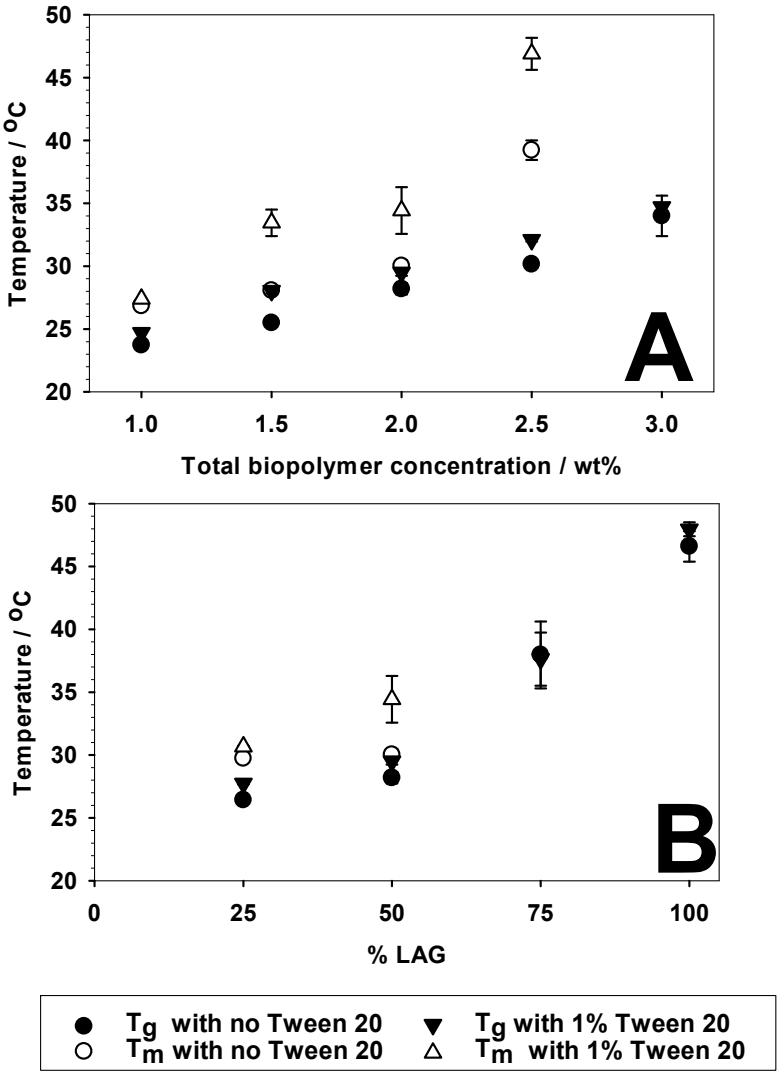

234

235 *Figure 1 - Gelling and melting temperature data for LAG/TSX samples. In figure A, the ratio of LAG:TSX was kept at 1:1 and*
236 *the total concentration of biopolymer was changed. In figure B, the total biopolymer concentration was kept constant at 2*
237 *wt% and the ratio of LAG:TSX was varied. Values given are mean averages from three measurements and error bars*
238 *represent standard deviation.*

239 Over the range of polymer blends tested, there was a strong positive correlation between the gelling
240 temperatures and the percentage of LAG (ρ = 0.97) however there were too few data points to
241 perform statistical analysis for the melting temperatures. The addition of 1 wt% Tween® 20 to these
242 samples, produced no statistical change in the phase transition temperatures of the LAG/TSX gels at a
243 constant biopolymer concentration (P(one-tail) = 0.49).

244 In summary, it was found that the only the total concentration of biopolymers was sensitive to the
245 addition of Tween® 20 with greater shifts in gelling and melting temperatures seen at higher total
246 polymer concentrations. In contrast, small increases in gelling and melting temperatures were seen
247 across all the blends tested, regardless of the polymer ratio.

248 For comparison, samples of 5 wt% gelatin with and without 1 wt% Tween® 20 were made, and the
249 measured gelling and melting temperatures were ca. 21.5 °C and 30.3 °C in each case, regardless of
250 the presence of surfactant. This data can be used to determine which, if any, of the LAG/TSX samples
251 would be potentially suitable as a gelatin replacement. Osorio *et al*. (2007) obtained gelling and
252 melting temperatures for gelatin using the crossover of the viscous and elastic moduli, and these
253 values are approximately 18 – 28 °C and 32 – 37 °C respectively, with thermal hysteresis values in the
254 order of ca. 10 °C: this agrees well with the measured values in our study.

255 ### *3.1.2 Frequency sweeps to determine the mechanical spectra*

256 Frequency sweeps were conducted to determine two important rheological parameters: the phase
257 angle (δ) and storage modulus (G'), and their dependence on the measurement frequency. This was
258 performed for the LAG/TSX gels with or without the addition of 1 wt% Tween® 20, and the results are
259 shown in Figure 2. A larger error bar indicates that the sample was more frequency-dependent, and
260 hence more liquid-like.

261 As the total concentration of biopolymer was increased – again, at a fixed blend of 50:50 LAG:TSX – a
262 steady decrease in the phase angle was seen (ρ = −0.95), dropping from ca. 20° at a concentration of
263 1 wt% to ca. 7° at a concentration of 3 wt%. The standard deviation in the phase angle significantly

decreased as the total biopolymer concentration was increased ($\rho = -0.91$), so the samples became less frequency-dependent. Conversely, the value of the storage modulus (G') increased exponentially ($\rho = 0.93$, $R^2 = 0.98$) as the total biopolymer concentration was increased, from ca. 30 Pa to ca. 1000 Pa. All of these data suggested that increasing the total concentration of biopolymer increased gel strength and made the gel more solid-like.

At a fixed biopolymer concentration of 2 wt%, the phase angle showed a steady increase from ca. 5° to ca. 13° from 25 to 75% LAG content, followed by a decrease as the blend reached 100% LAG back to ca. 7°, hence indicating that the gel was least solid-like at 75% LAG content. This was accompanied by an initial decrease in the value of the storage modulus of 300 Pa to 250 Pa from 25% to 50% LAG content, followed by another exponential increase to ca. 2000 Pa up to 100% LAG, hence indicating a minimum in gel strength was measured at 50% LAG. A negative second-order polynomial trendline showed good agreement for both the phase angle ($R^2 = 0.94$) and the storage modulus ($R^2 = 0.98$) with respect to percentage LAG content.

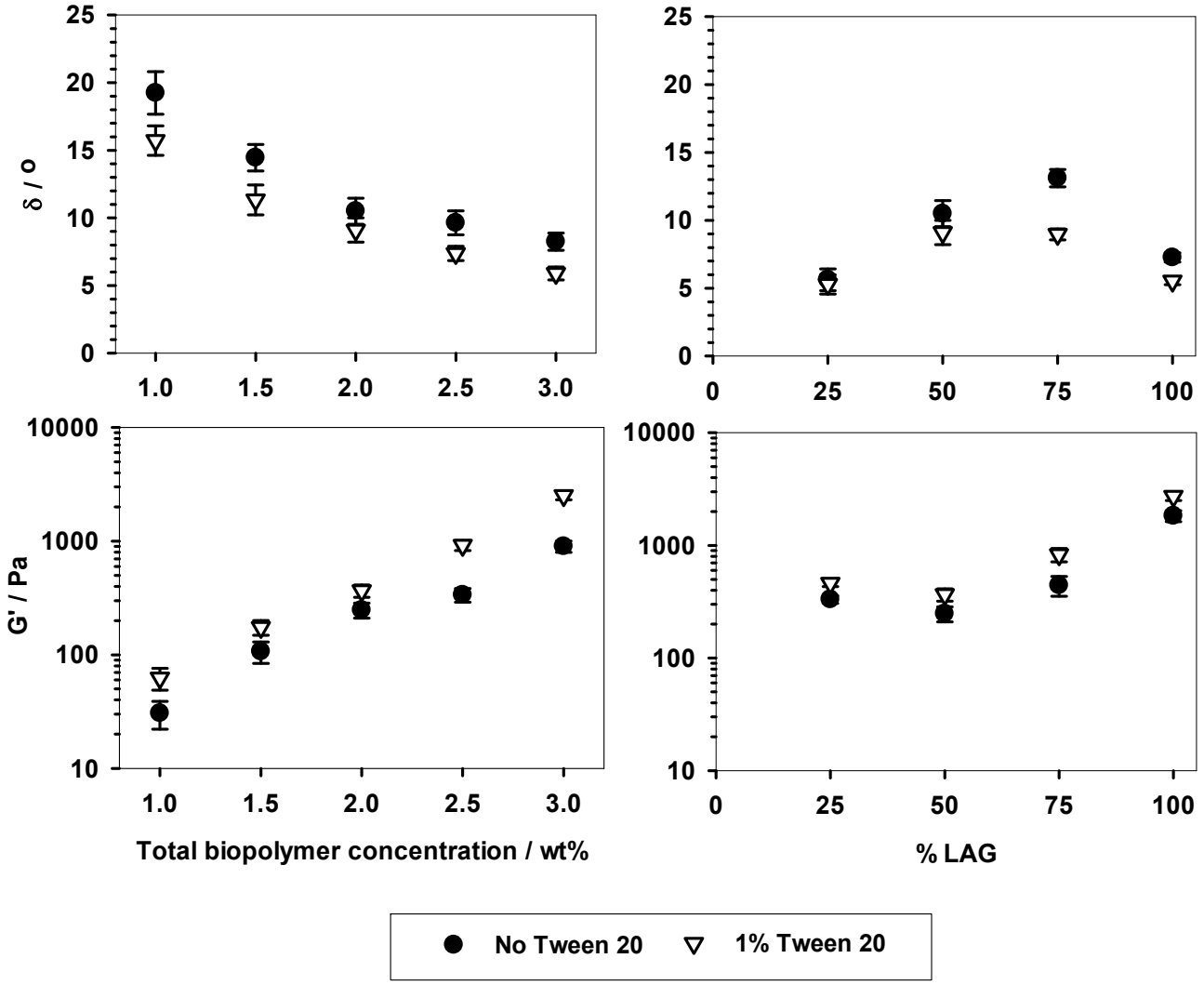

277

278 *Figure 2 - Frequency sweep data for LAG/TSX samples, plotting phase angle (δ) or elastic modulus (G') against formulation*
279 *parameters. Values given are mean averages from all data points in the three frequency sweeps, and error bars represent*
280 *standard deviation.*

281 The frequency dependence was low (SD ≤ 1°) in all blends tested, yet it was still found to correlate in
282 a strong negative relationship with the percentage of LAG (ρ = -0.97), indicating that the higher the
283 percentage of LAG in a blend, the less frequency dependent, and more solid-like, the gel was.

284 In the constant blend experiments, the addition of 1 wt% Tween® 20 led to statistically significant
285 decreases (P(one-tail) = 0.0014) in measured phase angles, in the order of 1 - 5°, compared to samples
286 without surfactant. There was some indication that the storage modulus increased upon addition of
287 Tween® 20 however these were found to be not statistically significant (P(one-tail) = 0.098). The size

of the reduction in phase angle upon addition of Tween® 20 was found to be mostly independent of the total biopolymer concentration (ρ = −0.64) in this case.

In the constant total polymer concentration experiments, the addition of Tween® 20 showed the largest decreases to the phase angle of LAG/TSX gels with the highest phase angle (ρ = 0.87): i.e., the largest change was seen for the 75% LAG, 25% TSX sample which had the largest starting phase angle. Furthermore, the magnitude of the increase in the storage modulus upon addition of Tween® 20 was found to be strongly dependent on both the percentage of LAG in the blend (ρ = 0.91) and the initial storage modulus (ρ = 0.97): the two are related. Hence, once again it is seen that the addition of surfactant had the greatest influence on the weaker, low thermal hysteresis gels compared to the stronger, high thermal hysteresis gels.

For comparison, frequency sweeps with formulations consisting of 5% gelatin with and without 1 wt% Tween® 20 were performed. It was found that the storage moduli were 360 ± 40 Pa and 445 ± 48 Pa, and the phase angles were 1.20 ± 0.43° and 1.17 ± 0.44° for the sample without and with Tween® 20 respectively. This provided a target storage modulus and phase angle for a gelatin replacement.

3.2 3D Printing

3.2.1 Rheology to predict printability

The printability of a range of LAG/TSX and gelatin gels was predicted using rheological data obtained from frequency sweeps. Phase angles (δ) and the relaxation exponents (m) can be used to predict the suitability of a material to being manufactured using a 3D printing process (Gholamipour-Shirazi, Norton, & Mills, 2019). One can obtain the relaxation component by noting the dependence of the elastic modulus (G') on angular frequency (ω) in a power-law relationship as shown in Equation 1 (Kavanagh & Ross-Murphy, 1998), using frequency sweep data. Previous work by Gholamipour-Shirazi, Norton and Mills (2019) showed that if $3° < \delta < 15°$ and $0.03 < m < 0.13$, the formulation was printable. The summary of printability results for LAG/TSX and LAG/TSX/Tween® 20 gels are shown in Tables 2A

– 2D. Formulations were stated to be 'feasibly printable' if the required rheological parameters were partially in the required range, and 'printable' if the parameters were fully in the required range, including any standard deviation. As can be seen, $R^2 \geq 0.95$ in all LAG/TSX samples, with and without surfactant, indicating a good fit to the power-law equation.

$$G'(\omega) \approx k_1 \omega^m \quad (1)$$

Table 2A – Table of rheological parameters used to determine printability based on the formula given in Equation 1. All samples consisted of a 50:50 blend of LAG:TSX whilst the total polymer concentration was varied. Values given are mean averages from three frequency sweeps with standard deviation. († = mean values are in the required range however printability is uncertain due to calculated error).

Total gelling biopolymer concentration (wt %)	δ (°)	k_1 (Pa s rad^{-1})	m	R^2	Printable?
1	19.24 ± 1.57	20.75 ± 0.87	0.190 ± 0.002	0.9990	No
1.5	14.45 ± 0.98	79.93 ± 2.96	0.14 ± 0.04	0.9992	No
2	10.50 ± 0.96	203.6 ±10.3	0.10 ± 0.05	0.9970	Yes†
2.5	9.42 ± 0.81	359.4 ± 16.2	0.09 ± 0.05	0.9964	Yes†
3	8.24 ± 0.64	811.1 ± 31.6	0.07 ± 0.04	0.9965	Yes

Table 2B – Table of rheological parameters used to determine printability based on the formula given in Equation 1. All samples consisted of 1 wt% Tween 20 with a 50:50 blend of LAG:TSX whilst the total polymer concentration was varied. Values given are mean averages from three frequency sweeps with standard deviation. († = mean values are in the required range however printability is uncertain due to calculated error).

Total gelling biopolymer concentration (wt %)	δ (°)	k_1 (Pa s rad^{-1})	m	R^2	Printable?
1	15.72 ± 1.09	51.91 ± 5.25	0.14 ± 0.10	0.9947	No
1.5	11.33 ± 1.10	152.9 ± 8.8	0.10 ± 0.06	0.9974	Yes†
2	9.10 ± 0.90	326.2 ± 13.4	0.083 ± 0.041	0.9968	Yes
2.5	7.38 ± 0.53	838.2 ± 29.1	0.068 ± 0.035	0.9967	Yes
3	5.90 ± 0.48	2334 ± 61	0.055 ± 0.03	0.9962	Yes

Table 2C – Table of rheological parameters used to determine printability based on the formula given in Equation 1. All were formulated at 2 wt% total gelling biopolymer concentration whilst ratio of LAG:TSX was varied. Values given are mean averages from three frequency sweeps with standard deviation. († = mean values are in the required range however printability is uncertain due to calculated error).

% LAG	δ (°)	k_1 (Pa s rad^{-1})	m	R^2	Printable?
100	7.26 ± 0.34	1578 ± 4	0.078 ± 0.002	0.9992	Yes
75	13.11 ± 0.64	336.8 ± 7.2	0.14 ± 0.02	0.9994	No
50	10.50 ± 0.96	203.6 ±10.3	0.10 ± 0.05	0.9970	Yes†
25	5.63 ± 0.80	302.7 ± 12.6	0.049 ± 0.042	0.9913	Yes

Table 2D – Table of rheological parameters used to determine printability based on the formula given in Equation 1. All were formulated with 1 wt% Tween 20 at 2 wt% total gelling biopolymer concentration whilst the ratio of LAG:TSX was varied. Values given are mean averages from three frequency sweeps with standard deviation.

% LAG	δ (°)	k_1 (Pa s rad^{-1})	m	R^2	Printable?
100	5.53 ± 0.27	2455 ± 6	0.057 ± 0.002	0.9972	Yes
75	8.96 ± 0.40	701.1 ± 9.1	0.092 ± 0.013	0.9992	Yes
50	9.10 ± 0.90	326.2 ± 13.4	0.083 ± 0.041	0.9968	Yes
25	5.28 ± 0.71	443.1 ± 16.6	0.043 ± 0.037	0.9900	Yes

Table 2E - Table of rheological parameters used to determine printability based on the formula given in Equation 1. All were formulated with 5 wt% gelatin whilst the concentration of Tween 20 was varied. Values given are mean averages from three frequency sweeps with standard deviation.

Concentration Tween 20 (wt %)	δ (°)	k_1 (Pa s rad^{-1})	m	R^2	Printable?
0	1.20 ± 0.43	518.6 ± 106.6	-0.040 ± 0.21	0.8730	No
1	1.17 ± 0.44	633.0 ± 124.6	-0.039 ± 0.203	0.8847	No

Upon addition of 1 wt% Tween 20 to the samples ascribed in Table 2A (Table 2B), the phase angle and the relaxation exponent decreased (P(one-tail) = 0.01), hence the samples became more printable. Without surfactant, formulations at 2 - 2.5 wt% total biopolymer concentration were feasibly printable and 3 wt% was predicted to be printable. Whereas upon addition of 1 wt% surfactant, 1.5 wt% samples were now feasibly printable, and printable at 2 wt% and beyond.

The ratio of biopolymers in the blend was also investigated to see if it influenced printability (Table 2C). It was discussed previously that the phase angle had a parabolic relationship with the percentage of LAG (at a constant total concentration of gelling biopolymers). In this case the parabolic behaviour can be seen to carry over, with 75% LAG being the only blend not deemed printable due to its high

mean phase angle. As previously, the addition of 1 wt% Tween 20 was investigated (Table 2D). Apart from the 25% LAG blend, both the phase angle relaxation exponent showed significant changes upon addition of Tween 20 (P(one-tail) = 0.04), and all samples became printable.

For comparison, a sample of 5 wt% gelatin with and without 1 wt% Tween 20 was investigated in an identical manner (Table 2E). It was found that the formulations were not printable since the phase angle and relaxation component were too small for the printing requirements.

3.2.2 3D printing of samples

Following the printability predictions, three LAG/TSX samples of varying formulation were tested for real-world printability. The samples tested were 0.5 wt% LAG/1.5 wt% TSX, 1.25 wt% LAG/1.25 wt% TSX, and – 1 wt% LAG/1 wt% TSX. Concentrations were chosen to represent a range of printability values within the permitted values for printability (Gholamipour-Shirazi et al., 2019). When comparing the predicted printability of the samples to the printed samples, shown in Figure 3, the images suggest that the rheological rules outlined by Gholamipour-Shirazi, Norton and Mills (2019) were generally a good indicator of printability. All samples were predicted to be printable, based on the value of the phase angle and the release exponent, however samples B and C could only be predicted to be feasibly printed because of the error in the measurements extended outside the printable parameters. In each

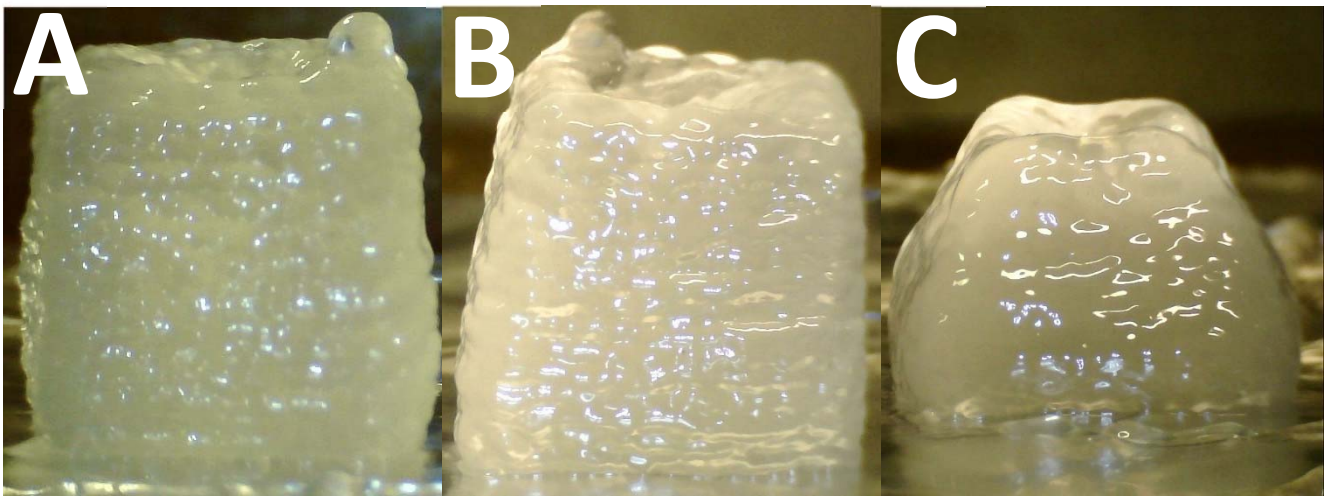

Figure 3 - Printed LAG/TSX samples. (A) – 0.5 wt% LAG/1.5 wt% TSX, (B) – 1.25 wt% LAG/1.25 wt% TSX, (C) – 1 wt% LAG/1 wt% TSX.

sample successful printing was achieved, with varying degrees of accuracy. Samples A and B were printed with good accuracy and the finished gel resembled a cube geometry. Sample C, did form a self-supporting gel, however it is clear that the gel sagged post-printing made evident by the narrowing of the cube nearer the top.

3.3 Measuring temperature-mediated release from moulded and printed gels

Following from the rheological data in section 3.1 and the printing data in 3.2, two LAG/TSX/Tween® 20 blends were chosen to represent potential gelatin replacements in release studies: these samples were 0.5 wt% LAG/1.5 wt% TSX/1 wt% Tween® 20 and 1 wt% LAG/1 wt% TSX/1 wt% Tween® 20. These concentrations were chosen because the measured melting temperatures were ca. 31 °C and 36 °C: at each extremity for the theoretical melting requirements of a gelatin replacement (greater than ambient temperature but below body temperature), and the storage moduli were very similar (within 100 Pa) of the measured storage modulus of 5 wt% gelatin with 1 wt% Tween® 20, hence the gel strength was similar. Additionally, based on the printing of samples in section 3.2.2, both samples were predicted to be printable and so the influence of moulding versus printing the samples on the release behaviour could be investigated. To this end, a sample of 0.5wt% LAG/1.5 wt% TSX/1 wt% Tween 20 was printed and compared to a moulded sample: all other samples in the release studies were moulded. The release profiles of the gels were measured in water at 20, 30 and 40 °C using conductivity, and the results are shown in Figure 4.

The 5 °C difference in melting temperatures between the two LAG/TSX blends led to significant differences in the release profiles. At 20 °C, the release time for both the gels was similarly slow (several hours), however, at 30 °C the 0.5 wt% LAG/1.5 wt% TSX/1 wt% Tween® 20 gel showed rapid melting behaviour, reaching a maximum conductivity value in under ten minutes, with 40 °C taking less than three minutes. Conversely, the 1 wt% LAG/1 wt% TSX/1 wt% Tween® 20 took over an hour to reach maximum conductivity at 30 °C, and under ten minutes at 40 °C.

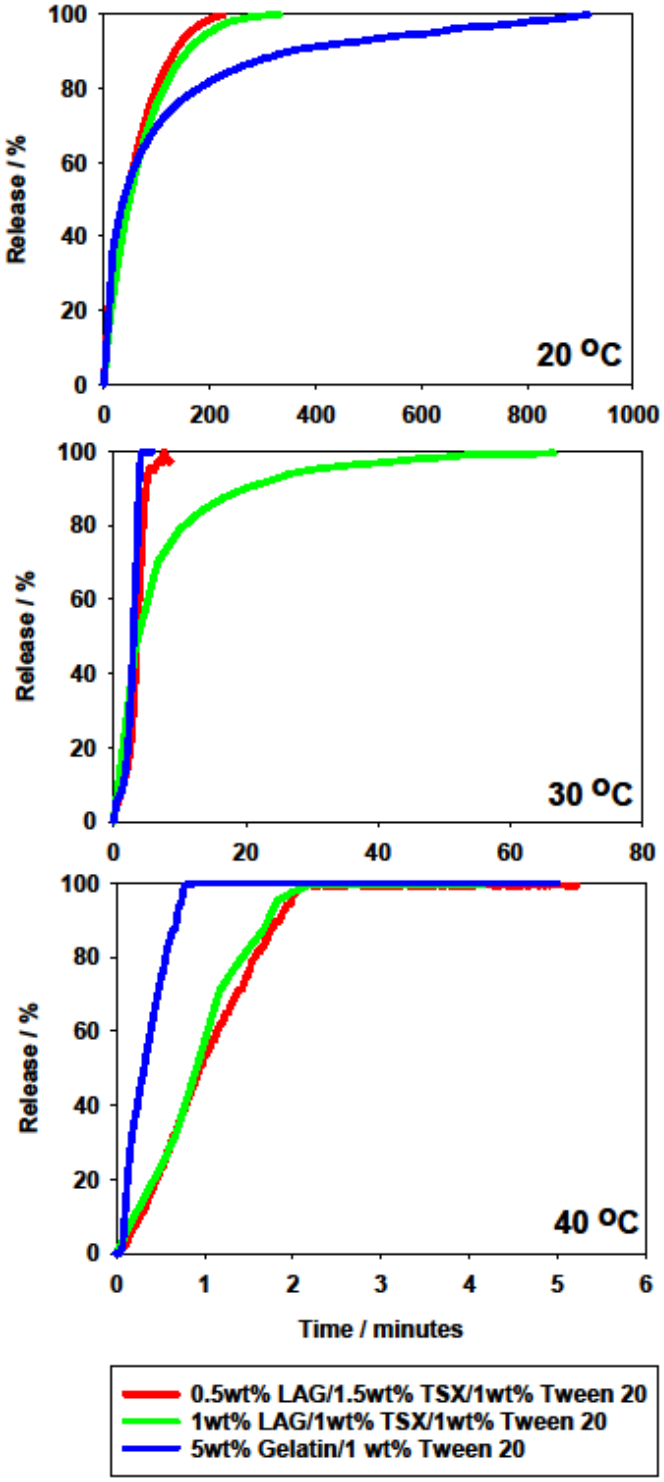

Figure 4 – Release data obtained from conductivity measurements of LAG/TSX/Tween and Gelatin/Tween Gels.

As a reference the release of 5 wt% gelatin with 1 wt% Tween® 20 was analysed in the same manner: release at 20 °C took nearly sixteen hours, yet at 30 °C and 40 °C maximum conductivity was achieved in approximately five minutes and one minute respectively.

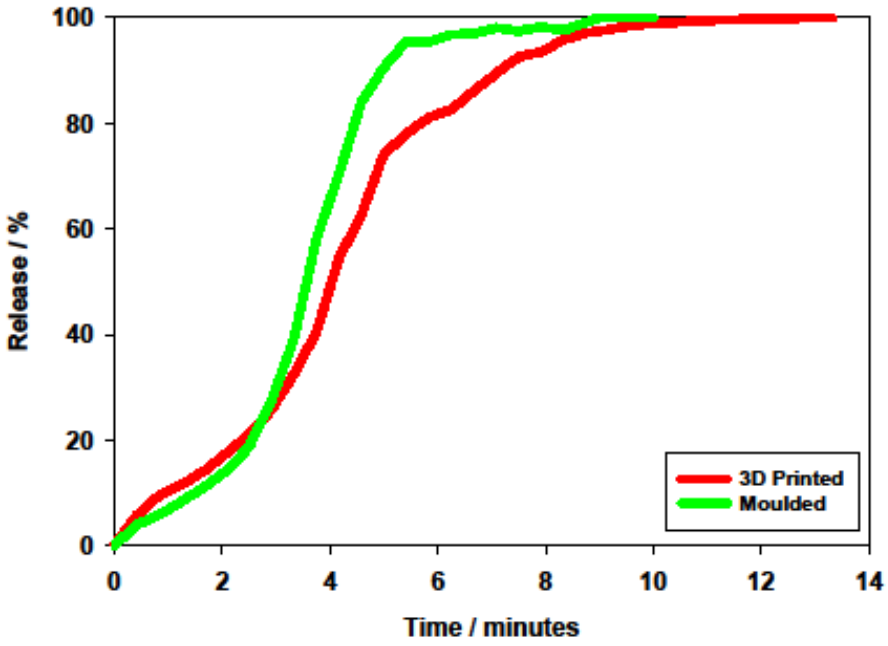

Figure 5 - A comparison of release data from a 3D printed and a moulded sample of 0.5wt% LAG/1.5wt% TSX/1wt% Tween® 20.

Furthermore, a comparison between gel samples manufactured using 3D printing and moulding was performed to see if the release profiles were similar, as shown in Figure 5. To this end, a sample of 0.5wt% LAG/1.5wt% TSX/1wt% Tween® 20 was prepared, printed and tested for release at 30 °C. The initial findings suggest that there was no statistical difference between the release profiles for the moulded gel and the printed gel. Further investigation between moulded and 3D printed samples was intended, however complications due to COVID-19 made further production of 3D printed samples unattainable for the foreseeable future.

4. Discussion

The rheological data in section 3.1 showed a statistically significant relationship that as the total biopolymer concentration was increased this led to a greater gelling temperature, melting

442 temperature, storage modulus and a lower phase angle. This is a common occurrence for many gelling
443 biopolymers that gel with a cation-driven helical-aggregation mechanism, such as kappa-carrageenan
444 or gellan. At a higher polymer concentration – and therefore gelling cation concentration – greater
445 aggregation of helices can take place, owing to better screening of repulsive charges on adjacent
446 helical aggregates. This leads to more thermally stable aggregates that can form at higher
447 temperatures and consequently need a higher temperature to overcome, explaining the greater
448 gelling and melting temperatures. The increased helical aggregation also explains the greater storage
449 modulus and lower phase angle as gel strength and solid-like character of the gels increases in such
450 circumstances. Similar rheological trends in gellan with polymer and cation concentration have been
451 reported by previous authors (Lee et al., 2011; Picone & Cunha, 2011).

452 The blend ratio, however, showed a more variable influence on the rheological properties of the gels.
453 The gelling temperature showed a strong positive correlation with LAG content: this is expected due
454 to the high gelling temperatures of LAG, and as the blend of LAG increased, the more LAG aggregates
455 can form. Hence it is predicted that the gelling temperatures are controlled by the LAG content. In
456 contrast, the storage modulus and phase angle had parabolic relationship with the LAG content, with
457 a maximum in phase angle achieved at 75% LAG and a minimum in storage modulus at 50% LAG. If
458 the morphology of the LAG/TSX was phase separated, one would expect a gradual decrease in phase
459 angle and an increase in storage modulus as the LAG content was increased, due to the fact that TSX
460 does not form a gel network on its own – such as the trends observed in the gelling temperature.
461 Therefore, the strong mechanical properties at 25% LAG content suggest the existence of some
462 coupled polymer network. Nevertheless, the purpose of this paper is not to unravel the mechanism
463 of LAG and TSX interactions, however these observations invoke some interesting questions.

464 In the constant blend experiments, the introduction of Tween® 20 to the LAG/TSX gel mixture led to
465 an increase in gelling temperature, melting temperature and storage modulus, and a reduction in the
466 phase angle and frequency dependence across the tested samples. Whereas in the constant total

biopolymer concentration experiments, only the frequency dependence and the magnitude of the increase in the storage modulus showed change upon the addition of Tween® 20. Pragmatically, this means that the total biopolymer concentration is the primary factor in determining the rheological properties of the gels, and the blend of LAG and TSX is secondary to this.

The alteration in rheological properties upon the addition of Tween® 20 is unlikely to simply be due to an increase in the effective concentration of the gelling biopolymers: an increase in polymer concentration by 1% would not explain the magnitude observed change in rheological behaviour. Volume exclusion effects could theoretically increase the effective polymer concentrations, however this is unlikely to be responsible for the shift in properties due because Tween® 20 micelles occupy a very similar volume to the equivalent mass of water that they replace, i.e. in micellar form, the density of Tween® 20 is very similar to that of water. Previous work concerning formulations of an anionic polymer with a non-ionic surfactant showed a similar increase in the gelling and melting temperature compared to the data reported here, and this was attributed to electrostatic shielding of the charged polymer helices by the surfactant micelles which enhanced helical aggregation (Fenton, Kanyuck, Mills, & Pelan, 2021; Yang & Pal, 2020). Fortunately, the magnitude of the increase in gelling, and more importantly, the melting temperatures was such that the LAG/TSX system could still be viable as a gelatin replacement.

Work set out in section 3.2, used the previously obtained rheological data to evaluate the printability of the samples. Generally, the samples found to be most printable were those whose total gelling biopolymer concentration was at least 2 wt%, or 1.5 wt% if 1 wt% Tween 20 was added. Printability was predicted to improve as biopolymer concentration was increased up to 3 wt%. Furthermore, printability was influenced by the LAG:TSX blend, with the 75% LAG blend being the least printable of all samples tested, and the 25% LAG blend the most printable. The addition of 1 wt% Tween® 20 improved the printability parameters of almost all samples tested, by decreasing the phase angle and the relaxation exponent and in no case did the printability parameters become less favourable. This is

likely because there was a small microstructural change upon the addition of Tween® 20, as discussed previously, and this simply led to samples which were more rheologically suited for a printing process. When examining the data for 5 wt% gelatin, it is clear that the samples were unprintable, hence the novelty of this formulation can be extended beyond providing similar mechanical and melting behaviours from a renewable, vegan formulation to being processible using additive manufacturing.

The significant difference in real-world printability between samples B & C is contrasted by their apparent similarities in both their measured phase angles and relaxation exponents, with differences of ca. 1° and 0.01 respectively, with both samples showing feasible printability. This suggests that the rules set out by Gholamipour-Shirazi, Norton and Mills (2019) successfully predicted if a sample was *at all* printable, but for samples that have printability parameters that are close to printability limits, the variability in rheological measurements make it difficult to successfully predict printability. Additionally, there may be another factor affecting the accuracy of the printed shape such as gelling temperature or gelation time. According to the measured values in section 3.1, sample B had a gelling temperature of ca. 2 °C higher than sample C: whether such a small difference in gelling temperature would lead to a marked difference in printability is debatable. If so, reducing the extrusion temperature or the bed temperature may improve the printability of samples with a lower gelling temperature.

The release profiles obtained in 3.3 are useful for indicating if the gel formulations could be suitable gelatin replacements, by seeing if they mimic the same melt-in-the-mouth behaviour that gelatin shows. From the release profiles obtained for the 5 wt% gelatin gel, it is clear that the requirement must be quick melting at 30 °C (under 10 minutes) and even quicker melting at 40 °C (1-2 minutes). Similar melting behaviour has been reported previously for gelatin (Mills, Spyropoulos, Norton, & Bakalis, 2011). At 20 °C, the release profiles for both of the moulded LAG/TSX gels was similarly slow – ca. 2-3 hours – and the release at this temperature for the LAG/TSX gels was driven mainly by diffusion of counter-ions out of the gel and subsequent erosion of the weakened gel layer. Slight

differences between different LAG/TSX blends arise at this temperature due to slightly different gel porosities and counter-ion concentrations within the gel, even though both gels have a melting temperature well above 20 °C. Gelatin, on the other hand, took significantly longer to show 100% release at 20 °C and that because the chemical nature of the gel network is markedly different: in the case of LAG/TSX, it relies on the existence of counter-ions to 'glue' the helices together in an aggregated network, and hence if these counter ions diffuse out of the gel in to water then the gel network collapses and is simply eroded from the outside, inwards, as diffusion of ions from the surface of the gel is much faster compared to diffusion from the bulk gel. As the gel is eroded this speeds up further diffusion of counter-ions from the gel by increasing the porosity of the gel and reducing the diffusion distance between counter-ions and the water. However, in the case of gelatin the movement of counter ions from the gel is pure-diffusion since there is no erosion, resulting in much slower diffusion (Mills et al., 2011). This mechanism of erosion in LAG/TSX versus pure diffusion in gelatin is further evidenced by the fact that at the end of the release experiments at 20 °C, there was no solid material left in the LAG/TSX experiments, whereas for gelatin there was no observable change in the physical dimensions of the gel compared to the start of the experiment. This diffusion-erosion mechanism is shown graphically in Figure 6. The results suggest that the 0.5 wt% LAG/1.5 wt% TSX polymer blend has a much more similar melting behaviour to gelatin compared to 1 wt% LAG/1 wt% TSX, because at 30 °C release was comparatively much slower in the latter blend, than the former, which was much closer to those results obtained for gelatin.

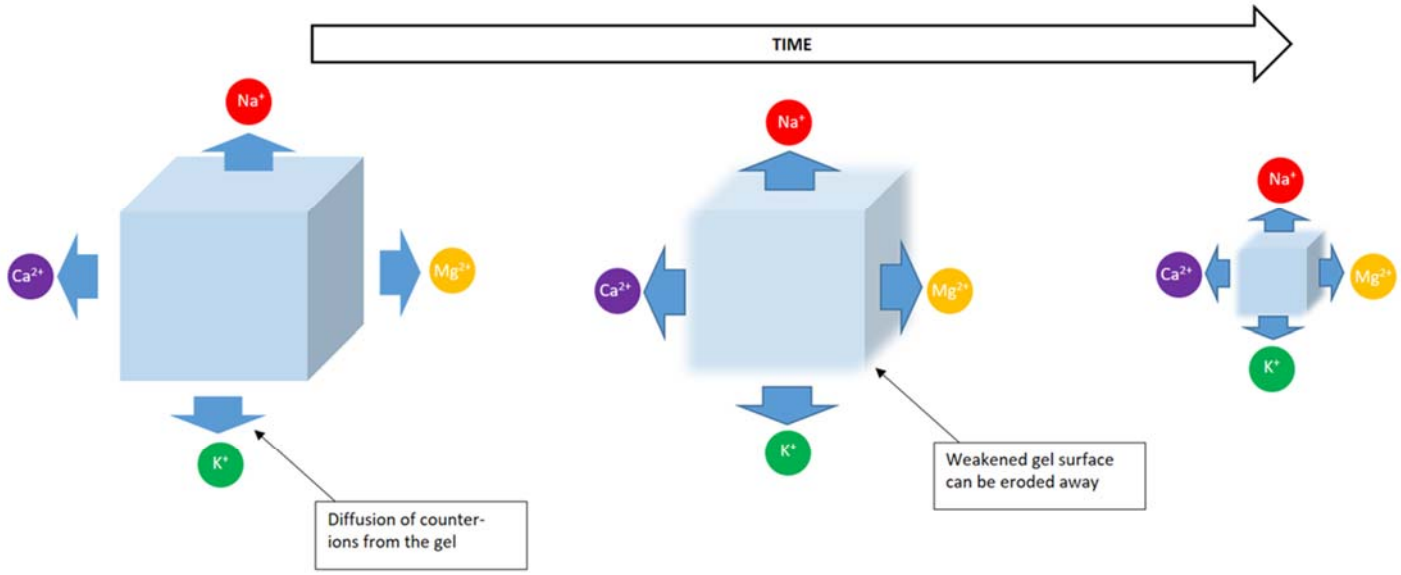

Figure 6 - Mechanism of erosion in LAG/TSX gels in water at temperatures below their melting temperature.

When comparing the release curves for a moulded sample compared to the 3D printed sample, the profiles are indistinguishable from one another, indicating that the 3D printing process did not significantly alter the structure of the final gel, and either technique could be used to manufacture gel samples. However, the authors recognise that further data in this area would be advantageous.

5. Conclusions

Overall these data have shown that the formulation engineering approach of a vegetarian gelatin replacement using low acyl gellan and tamarind see xyloglucan is possible. The most similar blend tested was 0.5 wt% LAG/1.5 wt% TSX, which showed very similar gel strength and melting behaviour to 5 wt% gelatin. Furthermore it was shown that LAG/TSX gels can be manufactured using 3D printing, whereas this is not possible for gelatin gels. The introduction of Tween® 20 to the LAG/TSX formulations had no detrimental effect on the printability of the LAG/TSX samples, and in many cases improved printability. Additionally, there was a small increase in the measured gelling and melting point temperatures which could influence efficacy in some applications if melting is required. The origin of these phenomena is currently unknown due to poor understanding of the mechanism of

LAG/TSX interactions and how the formation of the hybrid gel network forms and exactly what influence the surfactant has on the junction zones of the LAG/TSX system. Further work could involve more clearly elucidating the nature of this interaction with advanced imaging techniques such as scanning electron microscopy (SEM). The LAG/TSX system represents an exciting avenue for further research in to gelatin replacements.

6. Acknowledgements

We express our gratitude to the School of Chemical Engineering, University of Birmingham and the Engineering and Physical Sciences Research Council [grant number EP/N024818/1] for funding this research.

7. References

Chilvers, G. R., & Morris, V. J. (1987). Coacervation of gelatin-gellan gum mixtures and their use in microencapsulation. *Carbohydrate Polymers*, *7*(2), 111–120. https://doi.org/10.1016/0144-8617(87)90053-1

Daffner, K., Vadodaria, S., Ong, L., Nöbel, S., Gras, S., Norton, I., & Mills, T. (2021). Design and characterization of casein–whey protein suspensions via the pH–temperature-route for application in extrusion-based 3D-Printing. *Food Hydrocolloids*, *112*. https://doi.org/10.1016/j.foodhyd.2020.105850

Fasolin, L. H., Picone, C. S. F., Santana, R. C., & Cunha, R. L. (2013). Production of hybrid gels from polysorbate and gellan gum. *Food Research International*, *54*(1), 501–507. https://doi.org/10.1016/j.foodres.2013.07.026

Fenton, T., Kanyuck, K., Mills, T., & Pelan, E. (2021). Formulation and characterisation of kappa-carrageenan gels with non-ionic surfactant for melting-triggered controlled release. *Carbohydrate Polymer Technologies and Applications*, *2*, 100060.

https://doi.org/10.1016/j.carpta.2021.100060

Genot, C., Kabri, T. H., & Meynier, A. (2013). Stabilization of omega-3 oils and enriched foods using emulsifiers. In *Food Enrichment with Omega-3 Fatty Acids* (pp. 150–193). Elsevier Inc. https://doi.org/10.1533/9780857098863.2.150

Gholamipour-Shirazi, A., Norton, I. T., & Mills, T. (2019). Designing hydrocolloid based food-ink formulations for extrusion 3D printing. *Food Hydrocolloids*, *95*, 161–167. https://doi.org/10.1016/J.FOODHYD.2019.04.011

Godoi, F. C., Prakash, S., & Bhandari, B. R. (2016). 3d printing technologies applied for food design: Status and prospects. *Journal of Food Engineering*. https://doi.org/10.1016/j.jfoodeng.2016.01.025

Grasdalen, H., & Smidsrød, O. (1987). Gelation of gellan gum. *Carbohydrate Polymers*, *7*(5), 371–393. https://doi.org/10.1016/0144-8617(87)90004-X

Grisel, M., Aguni, Y., Renou, F., & Malhiac, C. (2015). Impact of fine structure of galactomannans on their interactions with xanthan: Two co-existing mechanisms to explain the synergy. *Food Hydrocolloids*, *51*, 449–458. https://doi.org/10.1016/j.foodhyd.2015.05.041

Ikeda, S., Nitta, Y., Kim, B. S., Temsiripong, T., Pongsawatmanit, R., & Nishinari, K. (2004). Single-phase mixed gels of xyloglucan and gellan. *Food Hydrocolloids*, *18*(4), 669–675. https://doi.org/10.1016/j.foodhyd.2003.11.005

Ikeda, S. and Talashek, T. A. (2007) *Low acyl gellan gels with reduced thermal hysteresis and syneresis*. United States Patent and Trademark Office Patent no. US 2009/0123628 A1. Available at: https://patents.google.com/patent/US20090123628A1/en (Accessed: 1 February 2021).

Jansson, P. E., Lindberg, B., & Sandford, P. A. (1983). Structural studies of gellan gum, an extracellular polysaccharide elaborated by Pseudomonas elodea. *Carbohydrate Research*, *124*(1), 135–139. https://doi.org/10.1016/0008-6215(83)88361-X

Kaur, H., Yadav, S., Ahuja, M., & Dilbaghi, N. (2012). Synthesis, characterization and evaluation of thiolated tamarind seed polysaccharide as a mucoadhesive polymer. *Carbohydrate Polymers*, *90*(4), 1543–1549. https://doi.org/10.1016/j.carbpol.2012.07.028

Kavanagh, G. M., & Ross-Murphy, S. B. (1998). Rheological characterisation of polymer gels. *Progress in Polymer Science*, *23*(3), 533–562. https://doi.org/10.1016/S0079-6700(97)00047-6

Kralova, I., & Sjöblom, J. (2009, October). Surfactants used in food industry: A review. *Journal of Dispersion Science and Technology*. https://doi.org/10.1080/01932690902735561

Kuo, M. S., Mort, A. J., & Dell, A. (1986). Identification and location of l-glycerate, an unusual acyl substituent in gellan gum. *Carbohydrate Research*, *156*, 173–187. https://doi.org/10.1016/S0008-6215(00)90109-5

Ledward, D. A. (2000). Gelatin. In G. O. Phillips & P. A. Williams (Eds.), *Handbook of Hydrocolloids* (2nd ed., pp. 67–86). Cambridge, UK: Woodhead Publishing Limited.

Lee, H., Fisher, S., Kallos, M. S., & Hunter, C. J. (2011). Optimizing gelling parameters of gellan gum for fibrocartilage tissue engineering. *Journal of Biomedical Materials Research - Part B Applied Biomaterials*, *98 B*(2), 238–245. https://doi.org/10.1002/jbm.b.31845

Mills, T., Spyropoulos, F., Norton, I. T., & Bakalis, S. (2011). Development of an in-vitro mouth model to quantify salt release from gels. *Food Hydrocolloids*, *25*(1), 107–113. https://doi.org/10.1016/j.foodhyd.2010.06.001

Moorhouse, R., Colegrove, G. T., Sandford, P. A., Baird, J. K., & Kang, K. S. (1981). PS-60: A New Gel-Forming Polysaccharide. In *ACS Symposium Series, Vol. 150* (pp. 111–124). American Chemical Society. https://doi.org/10.1021/bk-1981-0150.ch009

Morris, V. J. (1995). Synergistic Interactions with Galactomannans and Glucomannans. In S. E. Harding, S. E. Hill, & J. R. Mitchell (Eds.), *Biopolymer Mixtures* (pp. 289–314). Nottingham: Nottingham (United Kingdom) University Press.

626 Nayak, A. K., Pal, D., & Santra, K. (2014). Tamarind seed polysaccharide-gellan mucoadhesive beads
627 for controlled release of metformin HCl. *Carbohydrate Polymers*, *103*(1), 154–163.
628 https://doi.org/10.1016/j.carbpol.2013.12.031

629 Nishinari, K., Kim, B. S., Fang, Y., Nitta, Y., & Takemasa, M. (2006). Rheological and related study of
630 gelation of xyloglucan in the presence of small molecules and other polysaccharides. *Cellulose*,
631 *13*(4), 365–374. https://doi.org/10.1007/s10570-005-9041-0

632 Nitta, Y., Kim, B. S., Nishinari, K., Shirakawa, M., Yamatoya, K., Oomoto, T., & Asai, I. (2003). Synergistic
633 gel formation of xyloglucan/gellan mixtures as studied by rheology, DSC, and circular dichroism.
634 *Biomacromolecules*, *4*(6), 1654–1660. https://doi.org/10.1021/bm034103w

635 Osorio, F. A., Bilbao, E., Bustos, R., & Alvarez, F. (2007). Effects of concentration, bloom degree, and
636 pH on gelatin melting and gelling temperatures using small amplitude oscillatory rheology.
637 *International Journal of Food Properties*, *10*(4), 841–851.
638 https://doi.org/10.1080/10942910601128895

639 Picone, C. S. F., & Cunha, R. L. (2011). Influence of pH on formation and properties of gellan gels.
640 *Carbohydrate Polymers*, *84*(1), 662–668. https://doi.org/10.1016/j.carbpol.2010.12.045

641 Picone, C. S. F., & Cunha, R. L. (2013). Formation of nano and microstructures by polysorbate-
642 chitosan association. *Colloids and Surfaces A: Physicochemical and Engineering Aspects*, *418*,
643 29–38. https://doi.org/10.1016/j.colsurfa.2012.11.019

644 Warner, E. L., Norton, I. T., & Mills, T. B. (2019). Comparing the viscoelastic properties of gelatin and
645 different concentrations of kappa-carrageenan mixtures for additive manufacturing applications.
646 *Journal of Food Engineering*, *246*, 58–66. https://doi.org/10.1016/j.jfoodeng.2018.10.033

647 Yang, J., & Pal, R. (2020). Investigation of surfactant-polymer interactions using rheology and surface
648 tension measurements. *Polymers*, *12*(10), 1–20. https://doi.org/10.3390/polym12102302

649